Hindawi
Advances in Materials Science and Engineering
Volume 2022, Article ID 2178499, 6 pages
https://doi.org/10.1155/2022/2178499

Research Article

Mechanical Properties of Polyaniline/Polyvinyl Alcohol Composite Gels Utilized in Strain Sensor

X. Sun, W. J. Li, X. G. Li, C. J. Mi, and C. F. Zhang

School of Mechanical Engineering, Hunan University of Technology, Taishan Road, Tianyuan, Zhuzhou 412007, China

Correspondence should be addressed to C. J. Mi; michengji_86@126.com and C. F. Zhang; zhangchangfan@263.net

Received 21 October 2022; Revised 9 November 2022; Accepted 15 November 2022; Published 29 November 2022

Academic Editor: Jirapornchai Suksaeree

In order to determine the mechanical properties of polyaniline/polyvinyl alcohol composite gels used in strain sensors, both microstructure and macroscopic mechanics experiments are conducted on the specimen. Firstly, the preparation process for this material will be explained. Then, the microstructure of this material showing the wrinkles and small holes caused by water loss is discussed. Based on the static tension test, the final equivalent elastic coefficient and relaxation time are obtained. Then, the fatigue parameters like the asymptotic temperature increment, asymptotic dissipation, and energy tolerance to failure are determined by the thermal-graphic technique.

1. Introduction

The viscous goo is extremely easy to adhere to the surface of conveying mechanisms, and so adhesion resistance is produced [1, 2]. In order to overcome the interference of rheological properties from non-Newtonian fluids, a kind of polyaniline/polyvinyl alcohol composite gels used in strain sensors is proposed in this paper [3–7]. This kind of flexible sensor has a high piezoelectric ratio and good material toughness and anisotropy. Therefore, it could realize high-precision acquisition of multidimensional information and improve the control efficiency of viscous material transportation, which would provide technical support for the establishment of intelligent packaging equipment for thick sauce and viscous food [8–14].

Some researchers have focused on the composite hydrogel. Xu [15] suggested a kind of novel polyaniline/polyvinyl alcohol composite hydrogel which was made by the freezing-thawing and in-situ polymerization approach. The results showed that the polyaniline/polyvinyl alcohol composite hydrogel had good cytocompatibility and indicated that the composite hydrogel could be heated to about 23°C under sunlight with good hydrophilicity. Wang et al. stated that the graphene flexible pressure/strain sensor has better performance than the normal ones, like a wide measurement range, high sensitivity, and nano-size [16]. In order to solve the frequent failure of the conductive hydrogels based on the flexible sensors in a low-temperature environment, a novel fabrication of a freezing-tolerant and stretchable composite organohydrogel was presented by Xie et al. [17]. Zhang and Wang indicated that the polyvinyl alcohol hydrogels with anisotropic microstructures were first prepared by the directional freezing-thawing method to enhance the thermal stability and mechanical properties [18]. The anisotropic microstructures of the polyvinyl alcohol hydrogels were measured by scanning electron microscopy. The relatively regular orientation structure along the parallel direction was observed, and the uniform pore structure was found along the perpendicular direction as well. Shen et al. revealed that the mechanical properties of PVA/HA composite double-layer hydrogel were better than PVA/HA composite hydrogel, while the crosslink between PVA and HA would be enhanced through a casting drying approach [19]. The compression and stress relaxation tests of PVA/HA composite hydrogel were conducted on the specimens, and the stress relaxation curves and parameters were obtained as well [20]. However, few cyclic properties of the polyaniline/polyvinyl alcohol composite gels were found.

In this paper, the preparation of the polyaniline/polyvinyl alcohol composite gels is firstly explained. Then, based on the scanning electron microscopy, the topography of the

microstructure at low and high magnification is observed. Through the experimental work, the static tension properties, stress relaxation properties, and cyclic fatigue properties were all determined.

2. Material Preparation

The polyaniline-polyvinyl alcohol composite gels are made by the cyclic freezing/thawing in-situ polymerization method. Firstly, the polyvinyl alcohol is dissolved in a 2 mol/L hydrochloric acid solution at the temperature of 90°C, until it has a 15% polyvinyl alcohol solution. Then, 0.2 mL aniline is added to the solution to form 0.4 mol/L mixed liquid. At a temperature of 60°C, the mixed solution is stirred by magnetic forces for 4 hours to fully disperse. After that, the mixed liquid is frozen to a temperature of −30°C, lasting for 8 hours, and is thawed to be room temperature naturally. This process is repeated 5 times to obtain the polyvinyl alcohol original gel with dispersed aniline. Finally, the original gel is soaked in 1 mol/L ammonium persulfate solution to oxidize the aniline monomer, and the polyaniline/polyvinyl alcohol composite gels are obtained, as shown in Figure 1.

3. Microstructure

The microstructure of freeze-drying polyaniline/polyvinyl alcohol composite gels is investigated by SEM, as shown in Figure 2. The topography of microstructure at low magnification like in Figure 2(a), shows that wrinkles appear on the surface of composite gels, which is due to the microphase separation caused by the interpenetrating network structure when the network of the polyaniline-polyvinyl alcohol composite gels is obtained by the in-situ oxidation of the aniline monomer. The fine and even porous structure is investigated using a higher magnification, as shown in Figures 2(b) and 2(c). These small holes are created by the water loss after the gels are frozen and dried.

4. Static Mechanical Properties

Static tensile mechanical properties are the basic properties of the composite gels used in the flexible sensor. In order to estimate the rheological and elongation properties of the polyaniline/polyvinyl alcohol composite gels, static tension tests are conducted on the specimen, which has a width of 13 mm, a length of 24 mm, and thickness of 4 mm. The specimen is clamped in the rheometer (USA TA Co., Ltd., ARES-G2), as shown in Figure 3. Part 1 is the move module, part 2 is the movable gripping head, part 3 is the specimen, and part 4 is the fixed gripping head. The relaxing time in the stress relaxation test is determined to be 60 seconds. The first tensile speed is 0.1 mm/s, and the specimen is stretched to 29 mm in 50 seconds; the second tensile speed is 0.2 mm/s and the specimen is extended to 34 mm in 50 seconds as well. The stretching direction is parallel to the directional freezing orientation. The strain and stress history are shown in Figures 4(a) and 4(b), respectively. The calibration length of the measured specimen is 15 mm, and the maximum strain at two different load levels is 16.69% and 33.37%,

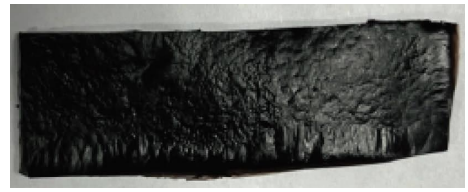

Figure 1: Sample of polyaniline/polyvinyl alcohol composite gels.

respectively. When the specimen is in the stress relaxation period, it can be seen in Figure 4(a) that the strain remains unchanged.

The stress history of composite gels is shown in Figure 4(b). When the material enters into the stress relaxation state, the stresses decrease gradually. The maximum stress after stretching 5 mm and 10 mm is 0.00986 MPa and 0.01962 MPa, respectively. Based on the two-parameter Maxwell model, the stress relaxation function could be described as follows [20]:

$$F(t) = LEe^{(-t/T)}, \tag{1}$$

where F is force history, L is the constant deformation, E is the elastic coefficient, t is testing time, and T is relaxation time

The loading force could be expressed as follows [20]:

$$F = \sigma S, \tag{2}$$

where S is cross section of the specimen and σ is the normal stress.

Then, the stress history can be changed as follows:

$$\sigma(t) = LKe^{(-t/T)}, \tag{3}$$

K is the equivalent elastic coefficient.

According to equation (3) and the data from the stress history in the stress relaxation period, the fitting parameters are obtained and shown in Table 1. From the stress relaxation tests at two different load levels, the rheological parameters in the first condition are close to the other ones. So, the final equivalent elastic coefficient and relaxation time are their averaged values 0.00198 MPa/mm and 109 seconds, respectively.

In order to find the relationship between stress and strain responses of the polyaniline-polyvinyl alcohol composite gels, the quasi-static tensile test is conducted on the specimen as well. The tensile speed is 0.1 mm/s, and the test is suspended when the maximum loading force is 2.75 N. The stress-strain curve is displayed in Figure 5. The maximum stress is 0.053 MPa. After the strain is 80%, the material appears into the plastic period, and the stress does not linearly increase. When the strain is close to 90%, the stress starts to gradually decrease until the test is in failure.

5. Fatigue Properties under Dynamic Cyclic Tension

In order to measure the sensitivity of the polyaniline-polyvinyl alcohol composite gels used in sensors, a novel experimental device is proposed in this paper, as shown in

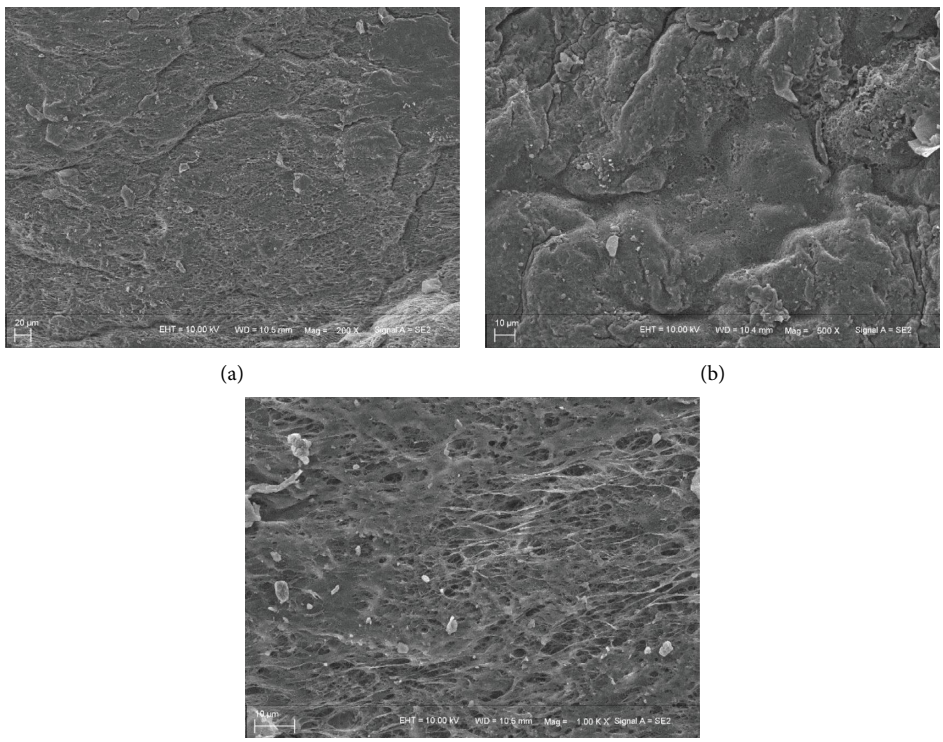

Figure 2: Microstructure of polyaniline/polyvinyl alcohol composite gels. (a) Microstructure of cross section under 200x, (b) microstructure of cross section under 500x, and (c) microstructure of cross section under 1000x.

Figure 3: Static tension of composite gels as measured by a rheometer.

Figure 6. In this picture, the part marked 1 is the controller, the part marked 2 is DC power, the part marked 3 is the fixed clamping head, and the part marked 4 is the testing specimen. The part marked 5 is the moveable clamping head, and the part marked 6 is a screw. The part marked 7 is an infrared thermography camera (USA Teledyne Co., Ltd., Flir), and the part marked 8 is a stepper motor. On this testing platform, both the loading frequency and stretching length for the specimen of the polyaniline-polyvinyl alcohol composite gels could be adjusted. Based on the infrared thermography technique, the temperature evolution of the material could be recorded by the camera under dynamic cyclic loadings. The dimensions of the specimen is a width of 20 mm, a length of 20 mm, and thickness of 4 mm. The testing speed is 8 mm/s at a room temperature of 16.46°C, and the loading frequency is 2 Hz.

The temperature evolution of composite gels under rapid monotonic tension is firstly shown in Figure 7. The temperature slightly increases with the movement of the clamping head at the beginning. When the stretching length is around 40 mm, the temperature rapidly increases to 17.82°C (the maximum temperature), which means the material is broken at a length of 51.8 mm. After that, the temperature decreases around the initial one.

A large number of literature have verified that the thermal evolution on the specimen surface under a certain level of stress amplitude could be divided into three stages, as shown in Figure 8, including the initial stage (marked stage I), the stable stage (marked stage II) and the final stage (marked stage III), respectively. The temperature in stage II is usually treated as a constant value from $N_{AS,0}$ to $N_{AS,f}$, and this period takes a remarkably predominant number of cycles.

For the sake of simplification, the asymptotic temperature increment θ_{AS} often is directly considered as a damage parameter for determining fatigue life. However,

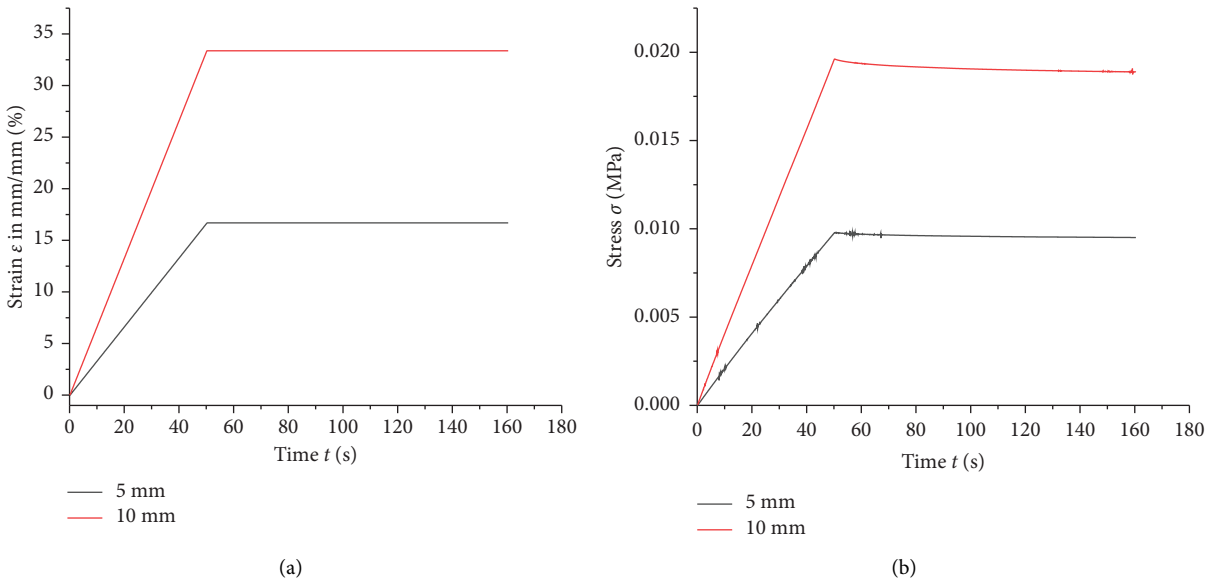

Figure 4: Mechanical responses of composite gels under stress relaxation: (a) strain history of composite gels under stress relaxation and (b) stress history of composite gels under stress relaxation.

Table 1: Rheological parameters.

Condition	Equivalent elastic coefficient K (MPa/mm)	Relaxation time T (s)	Regression coefficient R^2 (%)
Stretching 5 mm	0.001983	112.74	99.29
Stretching 10 mm	0.001977	105.26	97.70

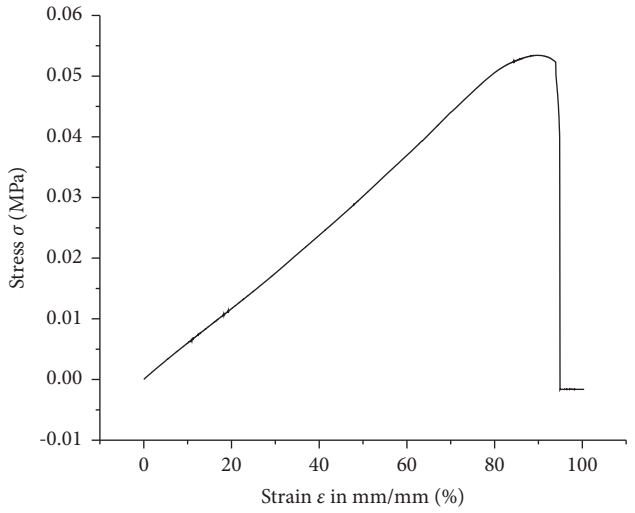

Figure 5: Stress and strain relationship of composite gels under static tension.

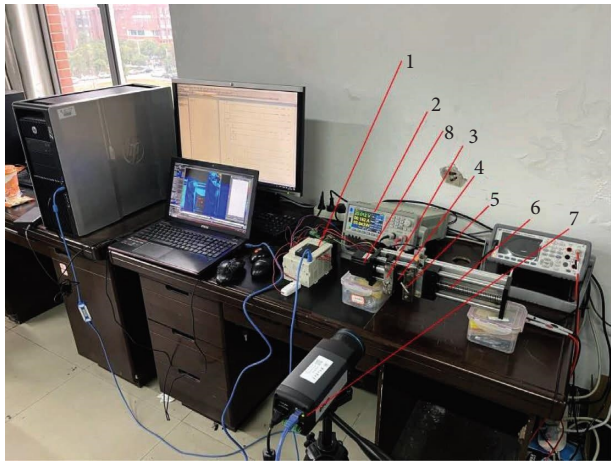

Figure 6: Fatigue tests platforms based on the thermal-graphic measurement.

the temperature variation is a kind of macro-manifestation and could not characterize inherent deformation mechanism under cyclic loading. The further relationship between physical parameter and fatigue damage evolution needs to be rebuilt. In the meantime, the temperature is extremely sensitive to heat exchange conditions. It is not reliable to achieve the fatigue indicator if external conditions are not properly considered. Therefore, the intrinsic dissipation is preferably considered as fatigue indicator for characterizing fatigue damage evolution law. Then, the intrinsic dissipation d_1 could be simplistically expressed as follows[21–24]:

$$\mathbf{d}_1 = \rho C\left(\frac{\partial\theta}{\partial t} + \frac{\theta}{\tau}\right), \tag{4}$$

where ρ is density, C is specific heat, θ is temperature increment with respect to the initial temperature, $\mathbf{t}$ is time, and τ stands for a time constant characterizing the heat loss. It is worth mentioning that the time parameter was ascertained by calculating the heat loss from the peak temperature to the room temperature.

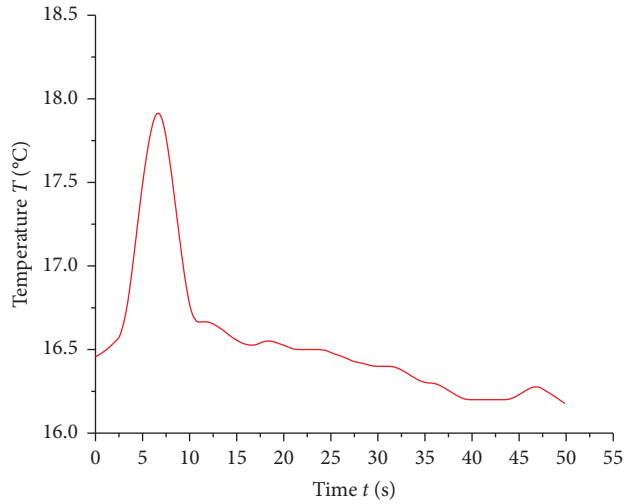

Figure 7: Temperature evolution of composite gels under rapid monotonic tension.

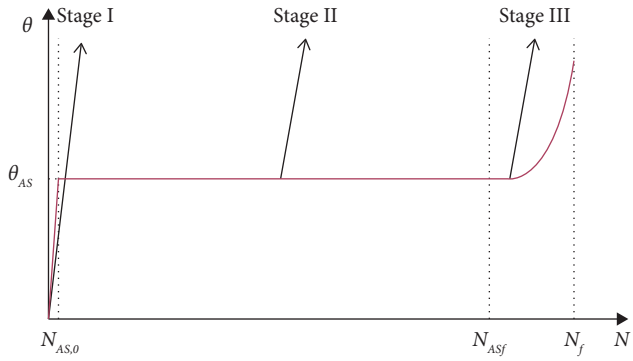

Figure 8: Schematic diagram of temperature evolution versus number of cycles during three stages.

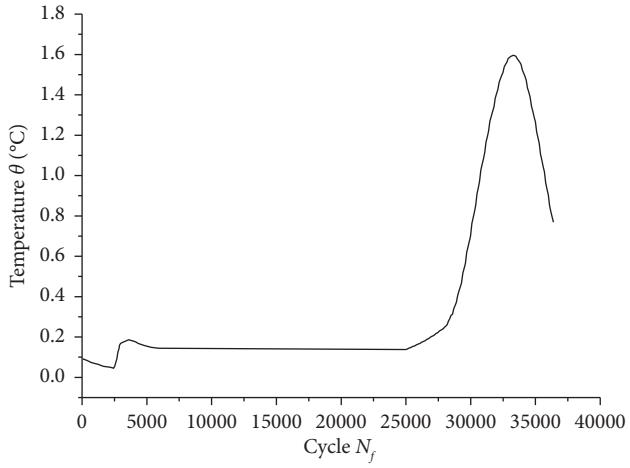

Figure 9: Temperature evolution of composite gels under cyclic tension.

Equation (4) shows the heat exchange with the environment is still taken into consideration by means of the parameter τ. When the temperature increment θ presents as an invariant value in stage II, the asymptotic temperature θ_{AS} could be used to express the asymptotic dissipation $d_{1,\mathrm{AS}}$ as the following equation [24]:

$$\mathbf{d}_{1,\mathrm{AS}} = \rho C \frac{\theta_{\mathrm{AS}}}{\tau}. \tag{5}$$

In this paper, the asymptotic dissipation $d_{1,\mathrm{AS}}$ is regarded as the fatigue indicator. In order to construct the relationship between the dissipated energy and number of cycles, the energy tolerance to failure E_C has to be defined. For the sake of convenience, the asymptotic dissipation per cycle $d_{1,\mathrm{AS}}/f$ ($f = N/\mathbf{t}$) is employed to replace the asymptotic dissipation per second $d_{1,\mathrm{AS}}$. In view of the above-mentioned characteristics shown in Figure 8, the lifespan in stage II ΔN_{AS} (is equal to $N_{\mathrm{AS,f}} - N_{\mathrm{AS},0}$) could be representative for the whole fatigue process $N_{\mathbf{f}}$, and then the energy tolerance to failure E_C could be expressed by [24–27]:

$$E_C = \int_0^{N_f} \frac{d_{1,\mathrm{AS}}}{f} \mathrm{d}N = \frac{d_{1,\mathrm{AS}}}{f} N_f. \tag{6}$$

In general, the energy tolerance to failure E_C means the ultimate ability to withstand cyclic loading, and it could be assumed to be constant for the same material regardless of loading modes. Once the asymptotic dissipation per cycle $d_{1,\mathrm{AS}}/f$ is calculated from the thermal evolution, the fatigue life $N_{\mathbf{f}}$ could be evaluated according to equation (6).

According to the tested data from the rapid monotonic tension, the cyclic properties are measured by the thermalgraphic technique as well. The applied cyclic stretching displacement is 45 mm at the frequency of 2 Hz, and there is no compression. The temperature increment with respect to the initial temperature is displayed in Figure 9. It can be found in Figure 9 that the thermal increment firstly declines in early stage I because of the tensile mean stress leading to the fall of temperature. Then, it decreases again at the starting of stage II. This phenomenon could be explained by a similar work-hardening mechanism that makes the material harder so that the corresponding strain becomes lower under the same external loading. And thus the plastic work reduces, as well as the dissipated energy. The test is suspended after 36389 cycles. The density ρ is 1803 kg/m^3, the specific heat C is 602 Jkg^{-1}K^{-1}, and the time constant τ is 12.5 s. Based on the experimental data, the asymptotic temperature increment θ_{AS} is 0.156°C. Then, according to (5) and (6), the asymptotic dissipation $d_{1,\mathrm{AS}}$ is 10350.66 J/m^3, and the energy tolerance to failure E_C is 1.88×10^8 J/m^3.

6. Conclusion

A kind of polyaniline-polyvinyl alcohol composite gels used in the strain sensor is fabricated by the cyclic freezing/thawing in-situ polymerization method. The microstructure of freeze-drying polyaniline/polyvinyl alcohol composite gels is investigated by SEM, which shows some small holes caused by the water loss. As measured by the stress relaxation testing, the rheological parameters such as the equivalent elastic coefficient and relaxation time are 0.00198 MPa/mm and 109 seconds, respectively. The stress-

strain relationship is also displayed under static tension in this paper. A novel experimental device is proposed to run the dynamic-cyclic tests. The cyclic properties are measured by the thermal-graphic technique, and fatigue parameters like the asymptotic temperature increment, asymptotic dissipation, and energy tolerance to failure are 0.156°C, 10350.66 J/m^3, and 1.88×10^8 J/m^3, respectively.

Data Availability

Data available in the following link https://en.cnki.com.cn/Article_en/CJFDTOTAL-CLDB201510018.htm.

Conflicts of Interest

All authors declare that there are no conflicts of interest.

Acknowledgments

This work was supported by the Natural Science Foundation of Hunan Province (2019JJ50116 and 2020JJ6078) and Hunan Provincial Education Department Innovation (CX20201030).

References

[1] G. W. Wang, J. Y. Wang, and R. Vivek, "Polyaniline nanoparticles: synthesis, dispersion and biomedical applications," *Mini-Reviews in Organic Chemistry*, vol. 14, no. 1, pp. 56–64, 2017.

[2] S. Bhadra, D. Khastgir, N. K. Singha, and J. H. Lee, "Progress in preparation, processing and applications of polyaniline," *Progress in Polymer Science*, vol. 34, no. 8, pp. 783–810, 2009.

[3] W. J. Yang, W. Y. Xu, X. Tao et al., "Two-stage thiol-based click reactions for the preparation and adhesion of hydrogels," *Polymer Chemistry*, vol. 11, no. 17, pp. 2986–2994, 2020.

[4] M. M. Liu, J. Li, and Z. G. Guo, "Polyaniline coated membranes for effective separation of oil-in-water emulsions," *Journal of Colloid and Interface Science*, vol. 467, pp. 261–270, 2016.

[5] Q. M. Jia, S. Y. Shan, L. H. Jiang, Y. M. Wang, and D. Li, "Synergistic antimicrobial effects of polyaniline combined with silver nanoparticles," *Journal of Applied Polymer Science*, vol. 125, no. 5, pp. 3560–3566, 2012.

[6] J. Zhou, Z. G. Lu, X. J. Zhu et al., "NIR photothermal therapy using polyaniline nanoparticles," *Biomaterials*, vol. 34, no. 37, pp. 9584–9592, 2013.

[7] N. B. Clark and L. J. Maher, "Non-contact, radio frequency detection of ammonia with a printed polyaniline sensor," *Reactive and Functional Polymers*, vol. 69, no. 8, pp. 594–600, 2009.

[8] H. Y. Mi, X. G. Zhang, S. D. Yang, X. G. Ye, and J. M. Luo, "Polyaniline nanofibers as the electrode material for supercapacitors," *Materials Chemistry and Physics*, vol. 112, no. 1, pp. 127–131, 2008.

[9] H. S. Kim, H. L. Hobbs, L. Wang, M. J. Rutten, and C. C. Wamser, "Biocompatible composites of polyaniline nanofibers and collagen," *Synthetic Metals*, vol. 159, no. 13, pp. 1313–1318, 2009.

[10] X. Zhang, H. S. Kolla, X. Wang, K. Raja, and S. K. Manohar, "Fibrillar growth in polyaniline," *Advanced Functional Materials*, vol. 16, no. 9, pp. 1145–1152, 2006.

[11] N. Bisht, A. Verma, S. Chauhan, and V. K. Singh, "Effect of functionalized silicon carbide nano-particles as additive in cross-linked PVA based composites for vibration damping application," *Journal of Vinyl and Additive Technology*, vol. 27, no. 4, pp. 920–932, 2021.

[12] R. Sanjay, P. Jyotishkumar, S. Suchart, and M. Ramesh, *Biodegradable Polymers, Blends and Composites*, pp. 309–326, Woodhead Publishing, London, UK, 2022.

[13] A. Verma, "A perspective on the potential material candidate for railway sector applications: PVA based functionalized graphene reinforced composite," *Applied Science and Engineering Progress*, vol. 15, no. 2, p. 5727, 2022.

[14] A. Verma, A. Parashar, and M. Packirisamy, "Atomistic modeling of graphene/hexagonal boron nitride polymer nano-composites: a review," *WIREs Computational Molecular Science*, vol. 8, no. 3, p. 1346, 2018.

[15] W. Y. Xu, "Fabrication and applications of polyaniline/polyvinyl alcohol composite gels," M.E. Thesis, Nanjing University of Posts and Telecommunications, Nanjing, China, 2020.

[16] Y. S. Wang, M. J. Zhang, and D. F. Liu, "Research program of graphene flexible pressure/strain sensors," *Measurement and Control Technology*, vol. 40, no. 11, pp. 39–47, 2021.

[17] Z. H. Xie, Z. P. Ma, Z. K. Xia et al., "Fabrication of a freezing-tolerant and stretchable composite organohydrogel for flexible strain sensors," *Packaging Journal*, vol. 13, no. 6, pp. 1–8, 2021.

[18] L. Zhang and H. L. Wang, "Preparation and property characterization of polyvinyl alcohol hydrogel with anisotropic structure," *Biomass Chemical Engineering*, vol. 53, no. 3, pp. 39–45, 2019.

[19] Y. Q. Shen, K. Chen, and Z. M. Dai, "Preparation and properties of PVA/HA composite double layer hydrogel," *Materials Review*, vol. 29, no. 5, pp. 73–77, 2015.

[20] Z. M. Dai, D. K. Zhang, and K. Chen, "Mechanical property analysis of PVA/HA composite hydrogel and its finite element simulation," *Journal of Medical Biomechanics*, vol. 27, no. 3, pp. 344–350, 2012.

[21] C. J. Mi, W. T. Li, X. W. Xiao, and F. Berto, "An energy-based approach for fatigue life estimation of welded joints without residual stress through thermal-graphic measurement," *Applied Sciences*, vol. 9, no. 3, pp. 397–411, 2019.

[22] D. Palumbo and U. Galietti, "Characterisation of steel welded joints by infrared thermographic methods," *Quantitative InfraRed Thermography Journal*, vol. 11, no. 1, pp. 29–42, 2014.

[23] O. A. Plekhov, N. Saintier, T. Palin-Luc, S. V. Uvarov, and O. B. Naimark, "Theoretical analysis, infrared and structural investigations of energy dissipation in metals under cyclic loading," *Materials Science and Engineering A*, vol. 462, no. 1-2, pp. 367–369, 2007.

[24] S. Dumoulin, H. Louche, O. S. Hopperstad, and T. Borvik, "Heat sources, energy storage and dissipation in high-strength steels: experiments and modelling," *European Journal of Mechanics - A: Solids*, vol. 29, no. 3, pp. 461–474, 2010.

[25] C. Doudard, S. Calloch, F. Hild, and S. Roux, "Identification of heat source fields from infrared thermography: determination of 'self-heating' in a dual-phase steel by using a dog bone sample," *Mechanics of Materials*, vol. 42, no. 1, pp. 55–62, 2010.

[26] N. Torabian, V. Favier, S. Ziaei-Rad, J. Dirrenberger, F. Adamski, and N. Ranc, "Thermal response of DP600 dual-phase steel under ultrasonic fatigue loading," *Materials Science and Engineering A*, vol. 677, pp. 97–105, 2016.

[27] A. Vshivkov, A. Iziumova, O. Plekhov, and J. Bär, "Experimental study of heat dissipation at the crack tip during fatigue crack propagation," *Frattura Ed Integrità Strutturale*, vol. 10, pp. 57–63, 2015.